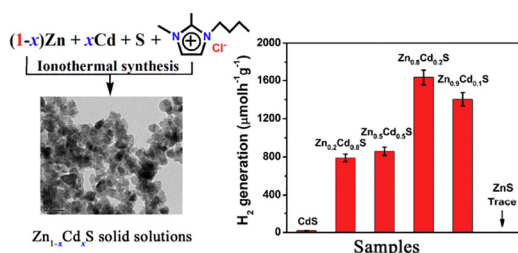


## Short communication

Ionochemical synthesis of  $Zn_{1-x}Cd_xS$  solid solutions with efficient photocatalytic  $H_2$  production via elemental-direct-reactionsMin-Ting Hao<sup>a,b</sup>, Qian-Qian Hu<sup>a,c,\*</sup>, Jian-Rong Li<sup>a,\*</sup>, Xiao-Ying Huang<sup>a</sup><sup>a</sup> State Key Laboratory of Structural Chemistry, Fujian Institute of Research on the Structure of Matter, Chinese Academy of Sciences, Fuzhou, Fujian 350002, People's Republic of China<sup>b</sup> College of Materials Science and Engineering, Fujian Normal University, Fuzhou, Fujian 350007, People's Republic of China<sup>c</sup> Key Laboratory of Optoelectronic Materials Chemistry and Physics, Chinese Academy of Sciences, Fuzhou, Fujian 350002, People's Republic of China

## GRAPHICAL ABSTRACT

A series of  $Zn_{1-x}Cd_xS$  ( $x = 0.1-0.9$ ) solid solutions with efficient photocatalytic  $H_2$  production were synthesized via elemental-direct-reactions under ionothermal conditions.

## ARTICLE INFO

## Keywords:

Solid solutions  
Ionochemical synthesis  
Elemental-direct-reaction  
Photocatalytic  $H_2$  production  
 $Zn_{1-x}Cd_xS$ 

## ABSTRACT

Photocatalytic hydrogen ( $H_2$ ) production from water splitting under visible-light irradiation is regarded as an attractive way to solve the energy crisis and environmental issues. In this communication, we report on a series of  $Zn_{1-x}Cd_xS$  ( $x = 0.1-0.9$ ) solid solutions synthesized via elemental-direct-reactions under ionothermal conditions. The as-synthesized samples were fully characterized by multiple techniques, revealing typically lamellar-like morphology and a gradual phase transition from cubic zinc blende to hexagonal Wurtzite structure with the increasing of Cd content in the solid solutions. Photocatalytic measurements indicate that the  $Zn_{0.8}Cd_{0.2}S$  solid solution presents the efficient photocatalytic activity for  $H_2$  generation rate of  $1635.6 \mu\text{mol}\cdot\text{h}^{-1}\cdot\text{g}^{-1}$ . This work illustrates that the ionothermal synthesis via elemental-direct-reaction routes is promising for preparing nanoscale functional chalcogenides on a large scale.

Since 1972 Fujishima and Honda first discovered that  $TiO_2$  could conduct photoelectrochemical water splitting under the UV light irradiation [1], the photocatalytic  $H_2$  evolution has attracted much attention because of the increasing energy crisis and environmental issues [2]. A large number of metal oxides and sulfides have been explored as photocatalysts for hydrogen production from water splitting [3]. The metal chalcogenides represented by CdS own more suitable band positions to harvest visible light compared with the oxides, thus, may

exhibit visible-light-driven  $H_2$  production activities [4]. However, in general the metal chalcogenides suffer from the low separation efficiency of photogenerated electrons ( $e^-$ ) and holes ( $h^+$ ) and low photocatalytic stability because of photo-corrosion [5]. To solve these problems, introducing Zn atoms into CdS to form  $Zn_{1-x}Cd_xS$  solid solutions is regarded as a viable method because ZnS and CdS possesses similar tetrahedron based structures and ZnS has the more negative conduction band [6]. Indeed,  $Zn_{1-x}Cd_xS$  solid solution photocatalysts

\* Corresponding authors.

E-mail addresses: [huqianqian@fjirsm.ac.cn](mailto:huqianqian@fjirsm.ac.cn) (Q.-Q. Hu), [jrli@fjirsm.ac.cn](mailto:jrli@fjirsm.ac.cn) (J.-R. Li).<https://doi.org/10.1016/j.inoche.2018.04.027>

Received 9 April 2018; Received in revised form 26 April 2018; Accepted 26 April 2018

Available online 30 April 2018

1387-7003/© 2018 Elsevier B.V. All rights reserved.

have been investigated extensively in the past decades due to the excellent performance in photocatalytic hydrogen production [7].

Tremendous efforts have been devoted to the synthesis of  $Zn_{1-x}Cd_xS$  solid solutions with a variety of sizes and morphologies to achieve high photocatalytic performance [8]. However, most of the synthetic routes require severe conditions such as high temperature and high pressure for crystallization, toxic agents [8a,8b,8d]. For instance, the typical hydro/solvothermal methods involve the use of inorganic metal salts and inorganic/organic sulfurs as the reactants. Apparently, it is still desired to develop a greener route to the synthesis of  $Zn_{1-x}Cd_xS$  solid solutions with high photocatalytic performance.

Ionic liquids (ILs) generally are organic salts with high thermal stability, no measurable vapor pressure, wide liquidus range and tunable solubility for many organic and inorganic species. The ILs has received ever growing attention owing to their ability to be an alternative of conventional organic solvents in many processes [9]. In particular, ILs can serve as an “all-in-one” solvent to simplify the reaction system, and even control the structures the final products [10]. Hence, the ionothermal synthesis involving the utilization of ILs as solvent and template represents a promising synthetic strategy in the synthesis of crystalline and nanostructured chalcogenides [11]. On the other hand, elemental-direct-reaction routes are the simplest and most straightforward reactions for synthesizing metal chalcogenide with the highest atom economy [12], while they are still scarce used in the reactions involving the ILs [13]. Recently Stucky et al. reported on the preparation of micro-/nanostructures chalcogenides from elemental precursors by using phosphonium-based ILs as the reaction media [13a]; while our group reported on the ionothermal synthesis of crystalline chalcogenides by elemental-direct-reactions in the imidazolium-based ILs [14].

Herein, we extended the application of ionothermal techniques to the synthesis of  $Zn_{1-x}Cd_xS$  solid solutions. The IL of 1-butyl-2, 3-dimethylimidazolium chloride ([Bmmim]Cl) was chosen as the reaction media to obtain a series of  $Zn_{1-x}Cd_xS$  solid solutions by elemental-direct-reactions of Zn/Cd and S. It is noted that such synthesis was accomplished at a relatively low temperature and low vapor pressure in a closed system and could be easily controlled, thus might be suitable for larger-scale synthesis.

The  $Zn_{1-x}Cd_xS$  solid solutions were obtained by the ionothermal reactions of metal Zn, metal Cd and elemental sulfur. The detailed procedures are given in the Supporting information (ESI). To identify the phase of the  $Zn_{1-x}Cd_xS$  solid solutions, powder X-ray diffraction (PXRD) patterns were recorded, and the results are shown in Fig. 1. The standard PXRD patterns of the bulk hexagonal Wurtzite CdS (JCPDS Card no. 65–3414) and the bulk cubic zinc-blende ZnS (JCPDS Card no. 65–1691) are also shown at the bottom and the top of Fig. 1, respectively. It can be seen that, as a small amount of Cd entered the ZnS crystals (e.g. the sample  $Zn_{0.9}Cd_{0.1}S$ ), the diffraction peaks of ZnS exhibit an obvious shift towards the lower angle but overall the experimental PXRD patterns are still comparable to that of cubic zinc-blende ZnS. With the further increasing of Cd content in the  $Zn_{1-x}Cd_xS$  solid solutions, the PXRD peak positions continuously shift to lower angle side, while the crystal phases of the  $Zn_{1-x}Cd_xS$  solid solutions gradually changed from the cubic zinc-blende to hexagonal Wurtzite structure and finally became the hexagonal Wurtzite CdS phase, implying the successful preparation of solid solutions instead of simple mixtures of ZnS and CdS [15]. On the basis of Bragg equation, the left shift of diffraction peaks is caused by the increase of lattice constants. Therefore, when  $Cd^{2+}$  (0.97 Å) partially replaces  $Zn^{2+}$  (0.74 Å) in ZnS lattice, the lattice constants of the obtained  $Zn_{1-x}Cd_xS$  are expanded, consequently resulting in the left shift of diffraction peaks.

Fig. 2 shows the representative scanning electronic microscopy (SEM), transmission electron microscopy (TEM) and high-resolution transmission electron microscopy (HRTEM) images of the  $Zn_{0.8}Cd_{0.2}S$  samples, which are composed of irregular micro-sheets with smooth surfaces, assembled by plentiful nanosheets with the sizes of 20–30 nm

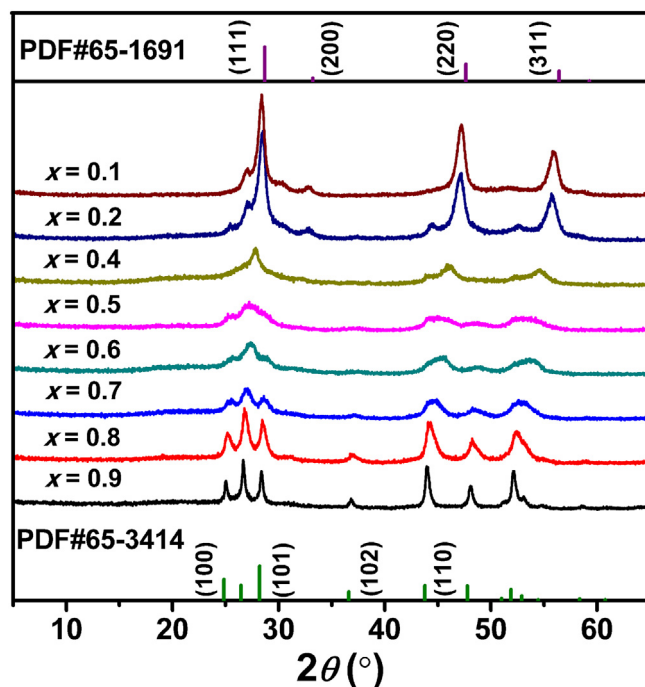


Fig. 1. PXRD patterns of  $Zn_{1-x}Cd_xS$  solid solutions compared with that of standard CdS and ZnS.

(Fig. 2(a)). In Fig. 2(c), it is clear that the nanosheets are single-crystalline and the lattices with a  $d$ -spacing of 3.1475 Å is observed for  $Zn_{0.8}Cd_{0.2}S$ , which is in between that of corresponding CdS and ZnS [8f,15]. From the image of selected area electron diffraction (SAED) (Fig. 2(d)), three diffraction rings close to the diffraction center with a spacing of 3.1475 Å, 1.9010 Å and 1.6463 Å correspond to the (111), (220) and (311) planes of zinc-blende phase, respectively [16], providing further evidence of the formation of  $Zn_{1-x}Cd_xS$  solid solution.

In order to understand the chemical states of Cd and Zn, the high resolution XPS spectra of Cd 3d, and Zn 3d core levels over the selected  $Zn_{1-x}Cd_xS$  solid solutions were investigated. As shown in Fig. 3a, the binding energies of Cd 3d<sub>5/2</sub> in the range of 405.18 eV–405.48 eV can be ascribed to the  $Cd^{2+}$  species [17]; in Fig. 3b, the binding energies of Zn 3d<sub>5/2</sub> in the range of 1021.88 eV–1022.98 eV are attributed to  $Zn^{2+}$  [18]. Moreover, the increase of  $x$  values results in the positive shift of binding energies of  $Cd^{2+}$  and the negative shift of binding energies of  $Zn^{2+}$ , again indicating the formation of a solid solution.

The solid state UV–Vis absorption spectra of Zn–Cd–S solid solutions are shown in Fig. 3c. The obvious red-shift from 2.78 eV to 2.26 eV can be seen in the absorption edge with increasing of the  $Cd^{2+}$  content, and consistently, the colors of the products change from incanus to yellow. As shown in Fig. S1 in ESI, Mott-Schottky (MS) curves illustrate that  $Zn_{0.4}Cd_{0.6}S$  and  $Zn_{0.9}Cd_{0.1}S$  are n-type semiconductor. It has been widely acknowledged that the flat band potential of an n-type semiconductor is about 0.10 V positive than the CB edge. In this way, the CB of  $Zn_{0.4}Cd_{0.6}S$  and  $Zn_{0.9}Cd_{0.1}S$  can be easily demonstrated as  $-0.776$  V and  $-1.155$  V (versus NHE), respectively. The gradual tendency implies that the band gaps of obtained solid solutions can be precisely tuned by varying the ratios of Cd/Zn, that is, solid solutions with precise band gaps can be obtained through the simple adjustment of the mass of reactant of Cd and Zn metals. The results of calculated band gap ( $E_g$ ) for  $Zn_{1-x}Cd_xS$  solid solutions, ZnS and CdS were obtained from the plots of  $(ah\nu)^2$  versus photon energy ( $h\nu$ ) using the relationship:  $ah\nu = A(h\nu - E_g)^n$ , where  $h\nu$  = photon energy,  $A$  = constant,  $\alpha$  = absorption coefficient, and  $n = 1/2$  for the allowed direct band gap;  $\alpha/S = (1 - R)^2/2R$ , where  $R$  is reflectivity,  $S$  is the scattering coefficient [16].

The photocatalytic reactivity for  $H_2$  evolution was evaluated in an

Download English Version:

<https://daneshyari.com/en/article/7748412>

Download Persian Version:

<https://daneshyari.com/article/7748412>

[Daneshyari.com](https://daneshyari.com)